Thermodynamics of quark quasi-particle ensemble

S. V. Molodtsov*
Joint Institute for Nuclear Research, Dubna, Moscow region, RUSSIA

G. M. Zinovjev
Bogolyubov Institute for Theoretical Physics, National Academy of Sciences of Ukraine, Kiev, UKRAINE
(Dated: February 5, 2022)

The features of hot and dense gas of quarks which are considered as the quasi-particles of the model Hamiltonian with four-fermion interaction are studied. Being adapted to the Nambu-Jona-Lasinio model this approach allows us to accommodate a phase transition similar to the nuclear liquid-gas one at the proper scale and to argue an existence of the mixed (inhomogeneous) phase of vacuum and normal baryonic matter as a plausible scenario of chiral symmetry (partial) restoration. Analyzing the transition layer between two phases we estimate the surface tension coefficient and speculate on the possible existence of quark droplet.

PACS numbers: 11.10.-z, 11.15.Tk

Notwithstanding the well-known incompletion of quantum chromodynamics (QCD) and its strongly limited capacity to perform the non-perturbative calculations both in the vacuum and at the finite temperature and baryonic density, one of the major predictions of this theory, a possible existence of quark-gluon plasma, was so exciting and convincing that pushed forward very active research programme in experiments with relativistic heavy ions. In such a situation when the applications which should usually be based on the standard interrelations between the hadronic properties and the QCD Lagrangian parameters are merely impossible, but the practical need in the quantitative estimates is dictated by the running experiments, we are forced to be very persistent and pragmatic in searching the effective Lagrangians.

The Nambu-Jona-Lasinio (NJL) model and its numerous extensions are the most popular in this context because they share some global symmetries of QCD and allow us to make surmountable some serious difficulties and uncertainties faced in the QCD calculations. It appears especially appreciable and effective in studying the nature of nuclear matter and its (super)dense state being treated as a model of QCD at large quark chemical potential. Nowadays the experiments in heavy-ion collisions to a considerable extent are driven by the results of phenomenological investigations of the properties of nucleon-nucleon force and the phase diagram of strongly interacting matter which relies on the corresponding estimates of experimentally measurable quantities.

Thus, exploring the QCD phase diagram with the effective models is targeted from the theoretical view point by necessity to find out some kind of interpolation between the physics as conceived by the lattice QCD simulations (still unrealistic because of several reasons) and the physics outputs of phenomenological studies. The vast activity (and progress) along this line [1] together with the recent experimental results from LHC and RHIC [2] lead to the unexpected vision of still pending questions and, perhaps, their new interpretation.

These and some related topics are discussed in this paper inspired by well known and fruitful idea about the specific role of surface degrees of freedom in the finite fermi-liquid systems [3] and, to a considerable extent, by our previous works [4], [5] in which the quarks were treated as the quasi-particles of the model Hamiltonian, and the problem of filling up the Fermi sphere was studied in detail. In particular, within the Nambu-Jona-Lasinio (NJL) model [6] new solution branches of the equation for dynamical quark mass as a function of chemical potential (the details are shown below in Fig. 1) have been found out. Besides, the existence and origin of the state filled up with quarks which is almost degenerate with the vacuum state both in the quasi-particle chemical potential and in the ensemble pressure has been demonstrated. In general, the approach developed may be considered as another microscopical substantiation of the bag model in which the states filled up with quarks might be instrumental as a 'construction material' for baryons.

Our analysis here is performed within two approaches which are supplementary, in a sense, but, fortunately, lead to the identical results. One of these approaches based on the Bogolyubov transformation is especially informative for studying the process of filling the Fermi sphere up because the density of quark ensemble develops a continuous dependence on the Fermi momentum in this case. It allows us to reveal an additional structure in the solution of gap equation for dynamical quark mass just in the proper interval of parameters characteristic for the phase transition and to trace its evolution. It results in the possibility for quark (fermionic) ensemble to be found in two aggregate states, a gas and a liquid, and the partial restoration of chiral condensate in a liquid phase (Section I). In order to make these conclusions easily perceptible we deal with the simplest version of the NJL model (with one flavor and one of the standard pa-

*Also at Institute of Theoretical and Experimental Physics, Moscow, RUSSIA

rameter sets). We try also to construct a description of transition layer between two phases and, in particular, to estimate the surface tension coefficient (Section II) what is of obvious importance in context of discussing the possible quark droplet formation (Section III). Some technical moments of calculating the mean energy functional are picked out into Appendix.

I. EXPLORING QUARK ENSEMBLE

Now as an input for starting we remind the key elements of approach which has been developed [4], [5]. The corresponding model Hamiltonian includes the interaction term taken in the form of a product of two colour currents located in the spatial points $\mathbf{x}$ and $\mathbf{y}$ which are connected by a form-factor and its density reads as

$$\mathcal{H} = -\bar{q}(i\gamma\nabla + im)q - \bar{q}t^a\gamma_\mu q \int d\mathbf{y}\bar{q}' t^b\gamma_\nu q' \langle A^a_\mu A'^b_\nu\rangle, \quad (1)$$

where $q = q(\mathbf{x})$, $\bar{q} = \bar{q}(\mathbf{x})$, $q' = q(\mathbf{y})$, $\bar{q}' = \bar{q}(\mathbf{y})$ are the quark and anti-quark operators,

$$q_{\alpha i}(\mathbf{x}) = \int \frac{d\mathbf{p}}{(2\pi)^3}\frac{1}{(2|p_4|)^{1/2}}\left[a(\mathbf{p},s,c)u_{\alpha i}(\mathbf{p},s,c)e^{i\mathbf{px}} + \right. \\ \left. + b^+(\mathbf{p},s,c)v_{\alpha i}(\mathbf{p},s,c)e^{-i\mathbf{px}}\right], \quad (2)$$

$p_4^2 = -\mathbf{p}^2 - m^2$, i–is the colour index, α is the spinor index in the coordinate space, a^+, a and b^+, b are the creation and annihilation operators of quarks and anti-quarks, $a\ |0\rangle = 0$, $b\ |0\rangle = 0$, $|0\rangle$ is the vacuum state of free Hamiltonian and m is a current quark mass. The summation over indices s and c is meant everywhere, the index s describes two spin polarizations of quark and the index c plays the similar role for a colour. As usual $t^a = \lambda^a/2$ are the generators of $SU(N_c)$ colour gauge group. The Hamiltonian density is considered in the Euclidean space and γ_μ denote the Hermitian Dirac matrices, $\mu,\nu = 1,2,3,4$. $\langle A^a_\mu A'^b_\nu\rangle$ stands for the form-factor of the following form

$$\langle A^a_\mu A'^b_\nu\rangle = \delta^{ab}\frac{2\ \widetilde{G}}{N_c^2-1}\left[I(\mathbf{x}-\mathbf{y})\delta_{\mu\nu} - J_{\mu\nu}(\mathbf{x}-\mathbf{y})\right], \quad (3)$$

where the second term is spanned by the relative distance vector and the gluon field primed denotes that in the spatial point $\mathbf{y}$. The effective Hamiltonian density (1) results from averaging the ensemble of quarks influenced by intensive stochastic gluon field A^a_μ, see Ref. [4]. For the sake of simplicity we neglect the contribution of the second term in (3) in what follows. The ground state of the system is searched as the Bogolyubov trial function composed by the quark-anti-quark pairs with opposite momenta and with vacuum quantum numbers, i.e.

$$|\sigma\rangle = \mathcal{T}\ |0\rangle\ , \\ \mathcal{T} = \Pi_{p,s}\exp\{\varphi[a^+(\mathbf{p},s)b^+(-\mathbf{p},s) + a(\mathbf{p},s)b(-\mathbf{p},s)]\}. \quad (4)$$

In this formula and below, in order to simplify the notations, we refer to one compound index only which means both the spin and colour polarizations. The parameter $\varphi(\mathbf{p})$ which describes the pairing strength is determined by the minimum of mean energy

$$E = \langle\sigma|H|\sigma\rangle\ . \quad (5)$$

By introducing the 'dressing transformation' we define the creation and annihilation operators of quasi-particles as $A = \mathcal{T}\ a\ \mathcal{T}^{-1}$, $B^+ = \mathcal{T}\ b^+\mathcal{T}^{-1}$ and for fermions $\mathcal{T}^{-1} = \mathcal{T}^\dagger$. Then the quark field operators are presented as

$$q(\mathbf{x}) = \int \frac{d\mathbf{p}}{(2\pi)^3}\frac{1}{(2|p_4|)^{1/2}}\ \left[\ A(\mathbf{p},s)\ U(\mathbf{p},s)\ e^{i\mathbf{px}} + \right. \\ \left. + B^+(\mathbf{p},s)\ V(\mathbf{p},s)\ e^{-i\mathbf{px}}\right]\ , \\ \bar{q}(\mathbf{x}) = \int \frac{d\mathbf{p}}{(2\pi)^3}\frac{1}{(2|p_4|)^{1/2}}\ \left[\ A^+(\mathbf{p},s)\ \overline{U}(\mathbf{p},s)\ e^{-i\mathbf{px}} + \right. \\ \left. + B(\mathbf{p},s)\ \overline{V}(\mathbf{p},s)\ e^{i\mathbf{px}}\right]\ ,$$

and the transformed spinors U and V are given by the following forms

$$U(\mathbf{p},s) = \cos(\varphi)\ u(\mathbf{p},s) - \sin(\varphi)\ v(-\mathbf{p},s)\ , \\ V(\mathbf{p},s) = \sin(\varphi)\ u(-\mathbf{p},s) + \cos(\varphi)\ v(\mathbf{p},s)\ . \quad (6)$$

where $\overline{U}(\mathbf{p},s) = U^+(\mathbf{p},s)\ \gamma_4$, $\overline{V}(\mathbf{p},s) = V^+(\mathbf{p},s)\ \gamma_4$ are the Dirac conjugated spinors.

In Ref. [5] the process of filling in the Fermi sphere with the quasi-particles of quarks was studied by constructing the state of the Sletter determinant type

$$|N\rangle = \prod_{|\mathbf{P}|<P_F;S} A^+(\mathbf{P};S)\ |\sigma\rangle\ , \quad (7)$$

which possesses the minimal mean energy over the state $|N\rangle$. The polarization indices run through all permissible values here and the quark momenta are bounded by the limiting Fermi momentum P_F. The momenta and polarizations of states forming the quasi-particle gas are marked by the capital letters similar to above formula and the small letters are used in all other cases.

As it is known the ensemble state at finite temperature T is described by the equilibrium statistical operator ξ. Here we use the Bogolyubov-Hartree-Fock approximation in which the corresponding statistical operator is presented by the following form

$$\xi = \frac{e^{-\beta\ \hat{H}_{\rm app}}}{Z_0}\ ,\quad Z_0 = {\rm Tr}\ \{e^{-\beta\ \hat{H}_{\rm app}}\}\ , \quad (8)$$

where an approximating effective Hamiltonian $H_{\rm app}$ is quadratic in the creation and annihilation operators of quark and anti-quark quasi-particles A^+, A, B^+, B and is defined in the corresponding Fock space with the vacuum state $|\sigma\rangle$ and $\beta = T^{-1}$. There is no need to know the exact form of this operator henceforth because all

the quantities of our interest in the Bogolyubov-Hartree-Fock approximation are expressed by the corresponding averages $n(P) = \mathrm{Tr}\{\xi A^+(\mathbf{P};S)A(\mathbf{P};S)\}$, $\bar{n}(Q) = \mathrm{Tr}\{\xi B^+(\mathbf{Q};T)B(\mathbf{Q};T)\}$ which are obtained by solving the following variational problem. The statistical operator ξ is defined by such a form in order to have the minimal value of mean energy of quark ensemble

$$E = \mathrm{Tr}\{\xi\ H\}$$

at the fixed mean charge

$$\bar{Q}_4 = \mathrm{Tr}\{\xi\ Q_4\} = V\ 2N_c \int \frac{d\mathbf{p}}{(2\pi)^3}\ [n(p) - \bar{n}(p)]\ , \quad (9)$$

where

$$Q_4 \ = \ -\int\ d\mathbf{x}\ \bar{q} i\gamma_4 q = \\ = \int \frac{d\mathbf{p}}{(2\pi)^3}\frac{-ip_4}{|p_4|}\left[A^+(p)A(p) + B(p)B^+(p)\right]\ ,$$

for the diagonal component (which is a point of our interest here) and at the fixed mean entropy ($S = -\ln\xi$)

$$\bar{S} = -\mathrm{Tr}\{\xi \ln\xi\} = \quad (10)$$
$$= -V2N_c \int \frac{d\mathbf{p}}{(2\pi)^3}\left[n(p)\ln n(p) + (1-n(p))\ln(1-n(p)) + \right.$$
$$\left. +\bar{n}(p)\ln\bar{n}(p) + (1-\bar{n}(p))\ln(1-\bar{n}(p))\right].$$

The mean charge (9) is calculated here up to the unessential (infinite) constant coming from permuting the operators BB^+ in the charge operator Q_4. It is appropriate here to remind that the mean charge should be treated in some statistical sense because it characterizes quark ensemble density and has no colour indices.The mean energy density per one quark degree of freedom $w = \mathcal{E}/(2N_c)$, $\mathcal{E} = E/V$ where E is a total energy of ensemble is calculated (the details of derivation can be found in Appendix) to get the following form

$$w = \int \frac{d\mathbf{p}}{(2\pi)^3}|p_4| + \int \frac{d\mathbf{p}}{(2\pi)^3}|p_4|\cos\theta[n+\bar{n}-1] - G\int \frac{d\mathbf{p}}{(2\pi)^3}\sin(\theta-\theta_m)\,[n+\bar{n}-1]\int \frac{d\mathbf{q}}{(2\pi)^3}\sin(\theta'-\theta'_m)\,[n'+\bar{n}'-1]I, \quad (11)$$

where $\theta = 2\varphi$, $\theta' = \theta(q)$, $n' = n(q)$, $I = I(\mathbf{p}+\mathbf{q})$ and the angle $\theta_m(p)$ is determined by $\sin\theta_m = m/|p_4|$. We are interested in minimizing the following functional

$$\Omega = E - \mu\ \bar{Q}_4 - T\ \bar{S}\ , \quad (12)$$

where μ and T are the Lagrange factors for the chemical potential and temperature respectively. The approximating Hamiltonian $\hat{H}_{\mathrm{app}}$ is constructed simply by using the information on $E - \mu\ \bar{Q}_4$ of presented functional (see, also below). For the specific contribution per one quark degree of freedom $f = F/(2N_c)$, $F = \Omega/V$ we receive

$$f = \int \frac{d\mathbf{p}}{(2\pi)^3}\ \left[|p_4|\cos\theta\ (n+\bar{n}-1) - \mu\ (n-\bar{n})\right] + \int \frac{d\mathbf{p}}{(2\pi)^3}\ |p_4| - G\int \frac{d\mathbf{p}}{(2\pi)^3}\ \sin(\theta-\theta_m)\ (n+\bar{n}-1)\times \\ \times\int \frac{d\mathbf{q}}{(2\pi)^3}\ \sin(\theta'-\theta'_m)\ (n'+\bar{n}'-1)\ I + T\int \frac{d\mathbf{p}}{(2\pi)^3}\ \left[n\ \ln n + (1-n)\ \ln(1-n) + \bar{n}\ \ln\bar{n} + (1-\bar{n})\ \ln(1-\bar{n})\right]\ . \quad (13)$$

The optimal values of parameters are determined by solving the following equation system ($df/d\theta = 0$, $df/dn = 0$, $df/d\bar{n} = 0$)

$$|p_4|\ \sin\theta - M\cos(\theta-\theta_m) = 0\ , \quad (14)$$
$$|p_4|\ \cos\theta - \mu + M\ \sin(\theta-\theta_m) - T\ \ln\left(n^{-1}-1\right) = 0\ ,$$
$$|p_4|\ \cos\theta + \mu + M\ \sin(\theta-\theta_m) - T\ \ln\left(\bar{n}^{-1}-1\right) = 0\ ,$$

where we denoted the induced quark mass as

$$M(\mathbf{p}) = 2G\int \frac{d\mathbf{q}}{(2\pi)^3}(1-n'-\bar{n}')\sin(\theta'-\theta'_m)\,I(\mathbf{p}+\mathbf{q}). \quad (15)$$

Turning to the presentation of obtained results in the form customary for the mean field approximation we introduce a dynamical quark mass M_q parametrized as

$$\sin(\theta-\theta_m) = \frac{M_q}{|P_4|}\ ,\quad |P_4| = (\mathbf{p}^2 + M_q^2(\mathbf{p}))^{1/2}\ , \quad (16)$$

and ascertain the interrelation between induced and dynamical quark masses. From the first equation of system

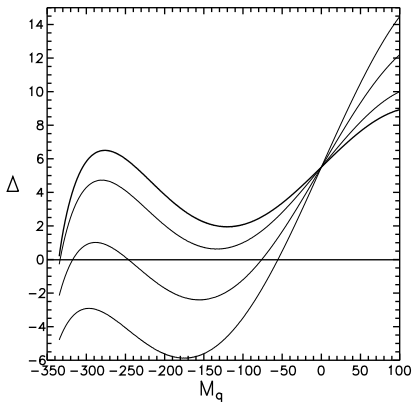

FIG. 1: The residual Δ for equation (15) is presented as a function of dynamical quark mass M_q (MeV) at zero value of temperature and the following values of chemical potential μ (MeV) — 335 (the lowest curve), 340, 350, 360 (the top curve).

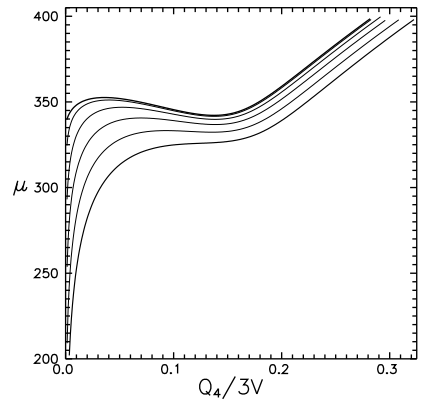

FIG. 2: The chemical potential μ (MeV) is plotted as a function of charge density $\mathcal{Q}_4 = Q_4/(3V)$ (in the units of ch/fm^3). The factor 3 relates the densities of quark and baryon matters. The top curve corresponds to the situation of zero temperature. The curves following down correspond to the temperature values $T = 10$ MeV, ... , $T = 50$ MeV with spacing $T = 10$ MeV.

(14) we fix the pairing angle

$$\sin\theta = \frac{p\ M}{|p_4||P_4|}$$

and making use the identity

$$(|p_4|^2 - M\ m)^2 + M^2 p^2 = [p^2 + (M-m)^2]\ |p_4|^2\ , \quad (17)$$

find out that

$$\cos\theta = \pm\frac{|p_4|^2 - m\ M}{|p_4||P_4|}\ .$$

For the sake of clarity we choose the upper sign 'plus'. Then, as an analysis of the NJL model teaches, the branch of equation solution for negative dynamical quark mass is the most stable one. Let us remember here we are dealing with the Euclidean metrics (though it is not a principal point) and a quark mass appears in the corresponding expressions as an imaginary quantity. Now substituting the calculated expressions for the pairing angle into the trigonometrical factor

$$\sin(\theta - \theta_m) = \sin\theta\ \frac{p}{|p_4|} - \cos\theta\ \frac{m}{|p_4|}$$

and performing some algebraic transformations we come to the relation

$$M_q(\mathbf{p}) = M(\mathbf{p}) - m\ . \quad (18)$$

In particular, the equation for dynamical quark mass (15) is getting the form characteristic for the mean field approximation

$$M = 2G\ \int \frac{d\mathbf{q}}{(2\pi)^3}\ (1 - n' - \bar{n}')\ \frac{M_q'}{|P_4'|}\ I(\mathbf{p}+\mathbf{q}). \quad (19)$$

The second and third equations of system (14) allow us to find the following expressions

$$n = \left(e^{\beta(|P_4|-\mu)} + 1\right)^{-1},\ \bar{n} = \left(e^{\beta\ (|P_4|+\mu)} + 1\right)^{-1}, \quad (20)$$

and, hence, the thermodynamic properties of our system, in particular, the pressure of quark ensemble

$$P = -\frac{dE}{dV}\ .$$

By definition we should calculate this derivative at constant mean entropy, $d\bar{S}/dV = 0$. This condition makes possible, for example, to calculate the derivative $d\mu/dV$, but the mean charge $\bar{Q}_4$ should not also change. In order to maintain it valid we introduce two independent chemical potentials — for quarks μ and for anti-quarks $\bar{\mu}$ (following Eq. (20) with the opposite signs). It leads also to the change $\mu \to \bar{\mu}$ in definition of $\bar{n}$ in Eq. (refnewden). This kind of description apparently allows us to treat even some non-equilibrium states of quark ensemble (but with losing a covariance similar to the situation which takes place in electrodynamics while one deals with electron-positron gas). Here we are interested in the unaffected balanced situation of $\bar{\mu} = \mu$. Then the corresponding derivative of specific energy dw/dV might be presented as

$$\frac{dw}{dV} = \int \frac{d\mathbf{p}}{(2\pi)^3}\left(\frac{dn}{d\mu}\frac{d\mu}{dV} + \frac{d\bar{n}}{d\bar{\mu}}\frac{d\bar{\mu}}{dV}\right)\Big[|p_4|\cos\theta -$$
$$-2G\sin(\theta-\theta_m)\int\frac{d\mathbf{q}}{(2\pi)^3}\sin(\theta'-\theta_m')\,(n'+\bar{n}'-1)I\Big]\ .$$

Now representing the trigonometric factors via dynamical quark mass and drawing Eq. (15) we obtain for the ensemble pressure

$$P = -\frac{E}{V} - V2N_c\int\frac{d\mathbf{p}}{(2\pi)^3}\left(\frac{dn}{d\mu}\frac{d\mu}{dV} + \frac{d\bar{n}}{d\bar{\mu}}\frac{d\bar{\mu}}{dV}\right)|P_4|. \quad (21)$$

The requirement of mean charge conservation

$$\frac{d\bar{Q}_4}{dV} = \frac{\bar{Q}_4}{V} + V2N_c\int\frac{d\mathbf{p}}{(2\pi)^3}\left(\frac{dn}{d\mu}\frac{d\mu}{dV} - \frac{d\bar{n}}{d\bar{\mu}}\frac{d\bar{\mu}}{dV}\right) = 0, \quad (22)$$

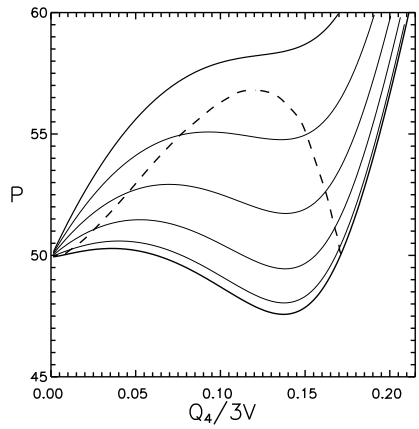

FIG. 3: The ensemble pressure P (MeV/fm^3) is shown as a function of charge density $\mathcal{Q}_4$ at temperatures $T = 0$ MeV, ... , $T = 50$ MeV with spacing $T = 10$ MeV. The lowest curve corresponds to zero temperature. The dashed curve shows the boundary of phase transition liquid–gas, see the text.

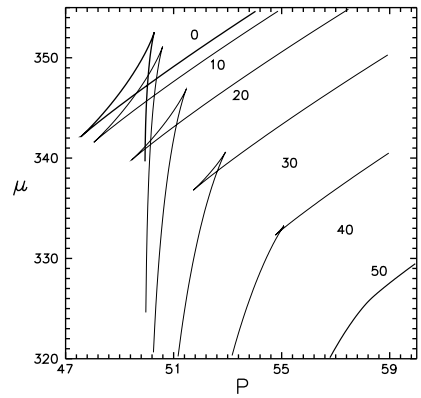

FIG. 4: The fragments of isotherms in Fig. 2, 3, see text. Chemical potential μ (MeV) is plotted as a function of pressure P MeV/fm^3. The top curve corresponds to the zero isotherm and following down with spacing 10 MeV till the isotherm 50 MeV (the lowest curve).

provides us with an equation which interrelates the derivatives $d\mu/dV$ and $d\bar{\mu}/dV$. Apparently, the regularized expressions for mean charge of quarks and antiquarks are meant (9) here. Dealing in a similar way with the requirement of mean entropy conservation, $d\bar{S}/dV = 0$, we receive another equation as

$$\int \frac{d\mathbf{p}}{(2\pi)^3} \frac{dn}{d\mu} \ln \frac{n}{1-n} \frac{d\mu}{dV} - \int \frac{d\mathbf{p}}{(2\pi)^3} \frac{d\bar{n}}{d\bar{\mu}} \ln \frac{\bar{n}}{1-\bar{n}} \frac{d\bar{\mu}}{dV} = = \frac{\bar{S}}{2N_c\, V^2} \ . \tag{23}$$

Substituting here $T \ln(n^{-1} - 1) = -\mu + |P_4|$ and $T \ln(\bar{n}^{-1} - 1) = \bar{\mu} + |P_4|$ we have after simple calculations with taking into account (22) that

$$\int \frac{d\mathbf{p}}{(2\pi)^3} \left(\frac{dn}{d\mu} \frac{d\mu}{dV} + \frac{d\bar{n}}{d\bar{\mu}} \frac{d\bar{\mu}}{dV} \right) |P_4| = -\frac{\bar{S}T}{2N_c V^2} - \frac{\bar{Q}_4 \mu}{2N_c V^2} \ .$$

Eventually it leads to the following expression for the pressure

$$P = -\frac{E}{V} + \frac{\bar{S}\ T}{V} + \frac{\bar{Q}_4\ \mu}{V} \ . \tag{24}$$

(of course, the thermodynamic potential is $\Omega = -P\ V$). At small temperatures the anti-quark contribution is negligible, and thermodynamic description can be grounded on utilizing one chemical potential μ only. If the antiquark contribution is getting intrinsic the thermodynamic picture becomes more complicated due to the necessity to obey the condition $\bar{\mu} = \mu$ which comes to the play. In particular, at zero temperature we might consider the anti-quark contribution absent and obtain

$$P = -\mathcal{E} + \mu\ \rho_q \ ,$$

where $\mu = \left(P_F^2 + M_q^2(P_F)\right)^{1/2}$, P_F is the Fermi momentum and $\rho_q = N/V$ is the quark ensemble density.

For lucidity of our view point we consider mainly the NJL model [6] in this paper, i.e. the correlation function (the form-factor in Eq. (3)) behaves as the δ-function in coordinate space. It is well known fact that in order to have an intelligent result in this model one needs to use a regularization cutting of the momentum integration in Eq. (13). We adjust the standard set of parameters [7] here with $|\mathbf{p}| < \Lambda$, $\Lambda = 631$ MeV, $m = 5.5$ MeV and $G\Lambda^2/(2\pi^2) = 1.3$. This set at $n = 0$, $\bar{n} = 0$, $T = 0$ gives for the dynamical quark mass $M_q = 335$ MeV. In particular, it may be shown the following representation of ensemble energy is valid at the extremals of functional (13)

$$\begin{aligned} E &= E_{vac} + 2N_c V \int^{\Lambda} \frac{d\mathbf{p}}{(2\pi)^3}\ |P_4|\ (n + \bar{n})\ , \\ E_{vac} &= 2N_c V \int^{\Lambda} \frac{d\mathbf{p}}{(2\pi)^3} (|p_4| - |P_4|) + 2N_c V \frac{M^2}{4G}, \end{aligned} \tag{25}$$

It is easy to understand this expression with the vacuum contribution subtracted looks like the energy of a gas of relativistic particles and antiparticles with the mass M_q and coincides identically with that calculated in the mean field approximation.

Let us summarize the results of this exercise. So, we determine the density of quark n and anti-quark $\bar{n}$ quasiparticles at given parameters μ and T from the second and third equations of system (14). From the first equation we receive the angle of quark and anti-quark pairing θ as a function of dynamical quark mass M_q which is handled as a parameter. Then at small temperatures, below 50 MeV, and value of chemical potentials of dynamical quark mass order, $\mu \sim M_q$, there are several branches of solutions of the gap equation. Fig. 1 displays the difference of right and left sides of Eq. (15) which is denoted by Δ at zero temperature and several values of chemical potential μ (MeV) = 335 (the lowest curve), 340, 350, 360 (the top curve) as a function of parameter M_q. The

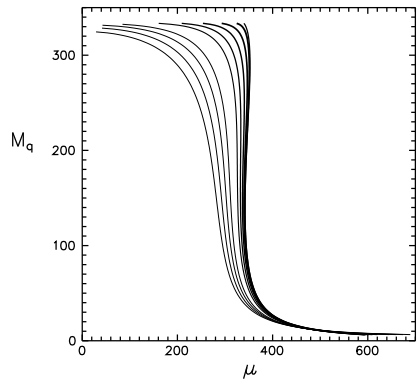

FIG. 5: The dynamical quark mass $|M_q|$ (MeV) is shown as a function of chemical potential μ (MeV) at the temperatures $T = 0$ MeV, ... , $T = 100$ MeV with spacing $T = 10$ MeV. The most right curve corresponds to zero temperature.

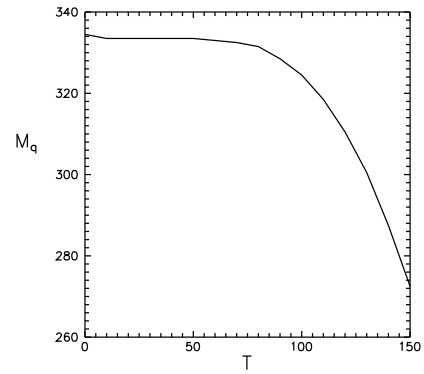

FIG. 6: The dynamical quark mass $|M_q|$ (MeV) as a function of temperature at the small value of charge density $\mathcal{Q}_4$.

zeros of function $\Delta(M_q)$ correspond to the equilibrium values of dynamical quark mass.

The evolution of chemical potential as a function of charge density $\mathcal{Q}_4 = Q_4/(3V)$ (in the units of charge$/fm^3$) with the temperature increasing is depicted in Fig. 2 (factor 3 relates the quark and baryon matter densities). The top curve corresponds to the zero temperature. The other curves following down have been calculated for the temperatures $T = 10$ MeV, ... , $T = 50$ MeV with spacing $T = 10$ MeV. As it was found in Ref. [5] the chemical potential at zero temperature is increasing first with the charge density increasing, reaches its maximal value, then decreases and at the densities of order of normal nuclear matter density[19], $\rho_q \sim 0.16/fm^3$, becomes almost equal its vacuum value. Such a behaviour of chemical potential results from the fast decrease of dynamical quark mass with the Fermi momentum increasing. It is clear from Fig. 2 the charge density is still multivalued function of chemical potential at the temperature slightly below 50 MeV. The Fig. 3 shows the ensemble pressure P (MeV/fm^3) as the function of charge density $\mathcal{Q}_4$ at several values of temperature. The lowest curve corresponds to the zero temperature. The other curves following up correspond to the temperatures $T = 10$ MeV, ... , $T = 50$ MeV (the top curve) with spacing $T = 10$ MeV. It is curious to remember now that in Ref. [5] the vacuum pressure estimate for the NJL model was received as 40—50 MeV/fm^3 which is entirely compatible with the results of conventional bag model. Besides, some hints at an instability presence (rooted in the anomalous behavior of pressure $dP/dn < 0$, see also [8], [9]) in some interval of the Fermi momentum has been found out.

Fig. 4 shows the fragments of isotherms of Fig. 2, 3 but in the different coordinates (chemical potential — ensemble pressure). The top curve is calculated at the zero temperature, the other isotherms following down correspond to the temperatures increasing with spacing 10 MeV. The lowest curve is calculated at the temperature 50 MeV. This plot obviously demonstrates that there are the states on the isotherm which are thermodynamically equilibrated and have an equal pressure and chemical potential (see the characteristic Van der Waals triangle with the crossing curves). The equilibrium points calculated are shown in Fig. 3 by the dashed curve. The points of dashed curve crossing with an isotherm pinpoint the boundary of gas—liquid phase transition. The corresponding straight line $P =$ const which obeys the Maxwell rule separates the non-equilibrium and unstable fragments of isotherm and describes a mixed phase. Then the critical temperature for the parameter which we are using in this paper becomes $T_c \sim 45.7$ MeV with the critical charge density as $\bar{Q}_4 \sim 0.12$ ch/fm^3. Usually the thermodynamic description is grounded on the mean energy functional which is the homogeneous function of particle number like $E = N\ f(S/N, V/N)$ (without vacuum contribution). It is clear such a description requires the corresponding subtractions to be introduced, however, this operation does not change the final results considerably. Now the vague arguments of Refs. [5] that the states filled up with quarks and separated from the instability region look like a 'natural construction material' to form the baryons are getting much more clarity and give a hope to understand the existing fact of equilibrium between vacuum and octet of stable (in strong interaction) baryons[20].

The dynamical quark mass $|M_q|$ (MeV) as a function of chemical potential μ (MeV) is presented for the temperatures $T = 0$ MeV, ... , $T = 100$ MeV with spacing $T = 10$ MeV in Fig. 5. The most right-hand curve corresponds to the zero temperature. At small temperatures, below 50 MeV, the dynamical quark mass is the multivalued function of chemical potential. Fig. 6 shows the dynamical quark mass as a function of temperature at small values of charge density $\mathcal{Q}_4 \sim 0$. Such a behaviour allows us to conclude that the quasi-particle size is getting larger with temperature increasing. It becomes clear if we remember that the momentum corresponding the maximal attraction between quark and anti-quark p_θ (according to Ref. [4]) is defined by $d\sin\theta/dp = 0$. In particular,

this parameter in the NJL model equals to

$$p_\theta = (|M_q|\ m)^{1/2}\ . \tag{26}$$

but its inverse magnitude defines the characteristic (effective) size of quasi-particle $r_\theta = p_\theta^{-1}$.

If one is going to define the quark chemical potential as an energy necessary to add (to remove) one quasi-particle (as it was shown in [5] at zero temperature), $\mu = dE/dN$, then in vacuum (i.e. at quark density ρ_q going to zero) quark chemical potential magnitude coincides with the quark dynamical mass. It results in the phase diagram displayed at this value of chemical potential although, in principle, this value could be smaller than dynamical quark mass as it has been considered in the pioneering paper [10]. If one takes, for example, chemical potential value equal to zero it leads to the conventional picture but, obviously, such a configuration does not correspond to the real process of filling up the Fermi sphere with quarks.

Apparently, our study of the quark ensemble thermodynamics produces quite reasonable arguments to propound the hypothesis that the phase transition of chiral symmetry (partial) restoration has been already realized as the mixed phase of physical vacuum and baryonic matter[21]. However, it is clear our quantitative estimates should not be taken as appropriate for comparing with, for example, the critical temperature of nuclear matter phase transition which has been experimentally measured and is equal 15–20 MeV. Besides, the gas component (at $T = 0$) has nonzero density (0.01 of the normal nuclear density) but in reality this branch should correspond to the physical vacuum, i.e. zero baryonic density[22]. In principle, an idea of global equilibrium of gas and liquid phases pursued us to put the adequate boundary conditions down at describing the transitional layer existing between the vacuum and the filled-up state and to calculate the surface tension effects. It looks plausible that the changes taking place in this layer could ascertain all ensemble processes similar to the theory of Fermi-liquids.

II. TRANSITION LAYER BETWEEN GAS AND LIQUID

This concept advanced would obtain the substantial confirmation if we are able to demonstrate an existence of this transition layer at which the ensemble transformation from one aggregate state to another takes place. As it was argued above the indicative characteristic to explore a homogeneous phase (at finite temperature) is the mean charge (density) of ensemble. It was demonstrated the other characteristics, for example, a chiral condensate, a dynamical quark mass, etc. could be reconstructed as well. So, here we are analyzing the transition layer at zero temperature.

If one assumes the parameters of gas phase are approximately the same as those at zero charge $\rho_g = 0$, i.e. as in vacuum (it means ignoring the negligible distinctions in the pressure, chemical potential and quark condensate), the dynamical quark mass develops the maximal value, and for the parameter choice of the NJL model it is $M = 335$ MeV. Then from the Van der Waals diagram one may conclude that the liquid phase being in equilibrium with the gas phase develops the density $\rho_l = 3 \times 0.185$ ch/fm^3 (by some reason which becomes clear below we correct it in favour of the value $\rho_l = 3 \times 0.157$ ch/fm^3). The detached factor 3 here links again the magnitudes of quark and baryon densities. The quark mass is approximately $\overset{*}{M} \approx 70$ MeV in this phase (and we are dealing with the simple one-dimensional picture hereafter).

The precursor experience teaches that an adequate description of heterogeneous states can be reached with the mean field approximation [12]. In our particular case it means making use the corresponding effective quark-meson Lagrangian [13] (the functional of Ginzburg-Landau type)

$$\begin{aligned}\mathcal{L} = -\bar{q}\ (\hat{\partial} + M)\ q - \frac{1}{2}\ (\partial_\mu \sigma)^2 - U(\sigma) - \\ -\frac{1}{4}\ F_{\mu\nu}F_{\mu\nu} - \frac{m_v^2}{2}\ V_\mu V_\mu - g_\sigma\ \bar{q}q\ \sigma + i g_v\ \bar{q}\ \gamma_\mu\ q\ V_\mu\ ,\end{aligned} \tag{27}$$

where

$$F_{\mu\nu} = \partial_\mu V_\nu - \partial_\nu V_\mu\ , \quad U(\sigma) = \frac{m_\sigma^2}{2}\ \sigma^2 + \frac{b}{3}\ \sigma^3 + \frac{c}{4}\ \sigma^4\ ,$$

and σ is the scalar field, V_μ is the field of vector mesons, m_σ, m_v are the masses of scalar and vector mesons and g_σ, g_v are the coupling constants of quark-meson interaction. The $U(\sigma)$ potential includes the nonlinear terms of sigma field interactions up to the fourth order. For the sake of simplicity we do not include the contribution coming from the pseudoscalar and axial-vector mesons.

The meson component of such a Lagrangian should be selfconsistently treated by considering the corresponding quark loops. (In terms of a relativistic extension of the Landau theory of Fermi-liquid the density fluctuations (meson field collective modes) are nothing more than the zero-sound as was shown in Ref. [9]). Here we do not see any reason to go beyond the well elaborated and reliable one loop approximation (27) [13], although recently the considerable progress has been reached (as we mention at the beginning of this paper) in scrutinizing the nonhomogeneous quark condensates by application of the powerful methods of exact integration [14]. Here we believe it is more practical to adjust phenomenologically the effective Lagrangian parameters basing on the transparent physical picture. It is easy to see that handling (27) in one loop approximation we come, in actual fact, to the Walecka model [15] but adopted for the quarks. In what follows we are working with the designations of that model and do hope it does not lead to the misunderstandings.

In the context of our paper we propose to interpret Eq. (27) in the following way. Each phase might be considered, in a sense, with regard to another phase as an

excited state which requires the additional (apart from a charge density) set of parameters (for example, the meson fields) for its complete description, and those are characterizing the measure of deviation from the equilibrium state. Then the crucial question becomes whether it is possible to adjust the parameters of effective Lagrangian (27) to obtain the solutions in which the quark field interpolates between the quasi-particles in the gas (vacuum) phase and the quasi-particles of the filled-up states. For all that the density of the filled-up state ensemble should asymptotically approach the equilibrium value of ρ_l and should turn to the zero value in the gas phase (vacuum).

The scale inherent in this problem may be assigned with one of the mass referred in the Lagrangian (27). In particular, we bear in mind the dynamical quark mass in the vacuum M. Besides, there are another four independent parameters in the problem and in order to compare them with the results of studying a nuclear matter we employ the form characteristic for the (nuclear) Walecka model

$$C_s = g_\sigma \ \frac{M}{m_\sigma} \ , \quad C_v = g_v \ \frac{M}{m_v} \ , \quad \bar{b} = \frac{b}{g_\sigma^3 \ M} \ , \quad \bar{c} = \frac{c}{g_\sigma^4} \ .$$

Taking the parameterization of the potential $U(\sigma)$ as $b_\sigma = 1.5 \ m_\sigma^2 \ (g_\sigma/M)$, $c_\sigma = 0.5 \ m_\sigma^2 \ (g_\sigma/M)^2$ we come to the sigma model but the choice $b = 0$, $c = 0$ results in the Walecka model. As to standard nuclear matter application the parameters b and c demonstrate vital model dependent character and are quite different from the parameter values of sigma model. Truly, in that case their values are also regulated by additional requirement of an accurate description of the saturation property. On the other hand, for the quark Lagrangian (27) we could intuitively anticipate some resemblance with the sigma model and, hence, could introduce two dimensionless parameters η and ζ in the form of $b = \eta \ b_\sigma$, $c = \zeta^2 \ c_\sigma$ which characterize some fluctuations of the effective potential. Then the scalar field potential is presented as follows

$$U(\sigma) = \frac{m_\sigma^2}{8} \ \frac{g_\sigma^2}{M^2} \ \left(4 \ \frac{M^2}{g_\sigma^2} + 4 \ \frac{M}{g_\sigma} \ \eta \ \sigma + \zeta^2 \sigma^2 \right) \ \sigma^2 \ .$$

The meson and quark fields are defined by the following system of the stationary equations

$$\begin{aligned} &\Delta \ \sigma - m_\sigma^2 \ \sigma = b \ \sigma^2 + c \ \sigma^3 + g_\sigma \ \rho_s \ , \\ &\Delta \ V - m_v^2 \ V = -g_v \ \rho \ , \\ &(\hat{\nabla} + \overset{*}{M}) \ q = (E - g_v \ V) \ q \ , \end{aligned} \tag{28}$$

where $\overset{*}{M} = M + g_\sigma \sigma$ is the running value of dynamical quark mass, E stands for the quark energy and $V = -iV_4$. The density matrix describing the quark ensemble at $T = 0$ has the form

$$\xi(x) = \int^{P_F} \frac{d\mathbf{p}}{(2\pi)^3} \ q_\mathbf{p}(x) \ \bar{q}_\mathbf{p}(x) \ ,$$

in which $\mathbf{p}$ is the quasi-particle momentum and the Fermi momentum P_F is defined by the corresponding chemical potential. The densities ρ_s and ρ at the right hand sides of Eq. (28) are by definition

$$\rho_s(x) = Tr \left\{ \xi(x), 1 \right\} \ , \quad \rho(x) = Tr \left\{ \xi(x), \gamma_4 \right\} \ .$$

Here we confine ourselves to the Thomas–Fermi approximation while describing the quark ensemble. Then the densities which we are interested in are given with some local Fermi momentum $P_F(x)$ as

$$\rho = \gamma \int^{P_F} \frac{d\mathbf{p}}{(2\pi)^3} = \frac{\gamma}{6\pi^2} \ P_F^3 \ , \tag{29}$$

$$\rho_s = \gamma \int^{P_F} \frac{d\mathbf{p}}{(2\pi)^3} \ \frac{\overset{*}{M}}{E} =$$

$$= \frac{\gamma}{4\pi^2} \ \overset{*}{M} \ P_F^2 \left\{ \left(1 + \lambda^2\right)^{1/2} - \frac{\lambda^2}{2} \ln \left[\frac{\left(1 + \lambda^2\right)^{1/2} + 1}{\left(1 + \lambda^2\right)^{1/2} - 1} \right] \right\},$$

where γ is the quark factor which for one flavour is $\gamma = 2N_c$ (N_c is the number of colours), $E = (\mathbf{p}^2 + \overset{*}{M}^2)^{1/2}$ and $\lambda = \overset{*}{M} / P_F$. By definition the ensemble chemical potential does not change and it leads to the situation in which the local value of Fermi momentum is defined by the running value of dynamical quark mass and vector field as

$$\mu = M = g_v \ V + \left(P_F^2 + \overset{*}{M}^2 \right)^{1/2} \ . \tag{30}$$

Now we should tune the Lagrangian parameters (27). For asymptotically large distances (in the homogeneous phase) we may neglect the gradients of scalar and vector fields and the equation for scalar field in the system (28) leads to the first equation which bounds the parameters C_s, C_v, $\bar{b}$, $\bar{c}$

$$\frac{M^2 (\overset{*}{M} - M)}{C_s^2} + \bar{b} \ M (\overset{*}{M} - M)^2 + \bar{c} (\overset{*}{M} - M)^3 = -\rho_s. \tag{31}$$

The asymptotic vector field is given by the ensemble density $V = C_v^2 \ \rho / (g_v M^2)$. The second equation results from the relation (30) for the chemical potential and gives

$$M = \frac{C_v^2 \ \rho}{M^2} + \left(P_F^2 + \overset{*}{M}^2 \right)^{1/2} \ . \tag{32}$$

Extracting the liquid density from (29) we obtain the Fermi momentum ($P_F = 346$ MeV) and applying the identities (31), (32) we have for the particular case $b = 0$, $c = 0$ that $C_s^2 = 25.3$, $C_v^2 = -0.471$, i.e. the vector component C_v^2 is small (comparing to C_s^2) and has negative value which is unacceptable. Apparently, it looks necessary to neglect the contribution coming from the vector field or to diminish the dynamical quark mass $\overset{*}{M}$ up to the value which retains the identity (32) valid with positive C_v^2 or equals to zero. In the gas phase the dynamical quark mass can also be corrected to the value larger than

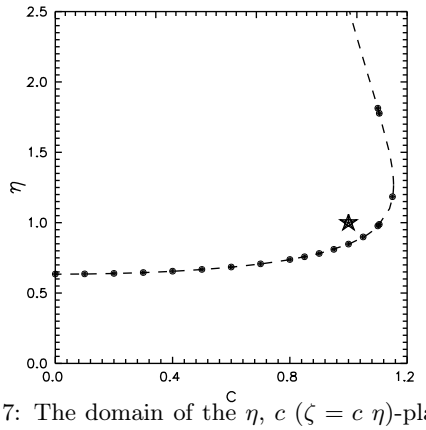

FIG. 7: The domain of the η, c ($\zeta = c\ \eta$)-plane in which an increase of specific energy occurs, see the text. The dots represent a stable kink. The star shows the position of canonical (chiral) kink, see the text.

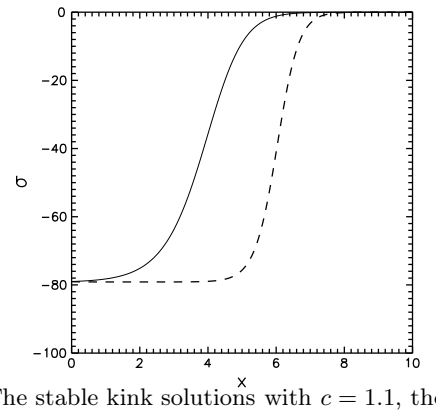

FIG. 8: The stable kink solutions with $c = 1.1$, the solid line corresponds to $\eta \approx 0.977$ ($m_\sigma \approx 468$ MeV) and the dashed line corresponds to $\eta \approx 1.813$ ($m_\sigma \approx 690$ MeV), x is given in the units of fm and σ is given in MeV.

the vacuum value. It is clear that in the situation of the liquid with the density $\rho_l = 3 \times 0.185$ ch/fm^3 the dynamical quark mass should coincide (or exceed) $M = 346$ MeV in the gas phase. However, here we correct the liquid density (as it was argued above) to decrease its value up to $\rho_l = 3 \times 0.157$ ch/fm^3 which is quite acceptable in the capacity of normal nuclear matter density. In fact, this possibility can be simply justified by another choice of the NJL model parameters. Thus, we obtain at $\overset{*}{M}= 70$ MэB and $b = 0$, $c = 0$ that $C_s^2 = 28.4$, $C_v^2 = 0.015$, i.e. we have a small but positive value for the vector field coefficient. At the same time, being targeted here to estimate the surface tension effects only we do not strive for the precise fit of parameters. In the Walecka model these coefficients are $C_s^2 = 266.9$, $C_v^2 = 145.7$, ($b = 0$, $c = 0$). Moreover, there is another parameter set with $C_s^2 = 64.$, $C_v^2 \approx 0$ [16] but it is rooted in an essential nonlinearity of the sigma-field due to the nontrivial values of the coefficients b and c. The option (formally unstable) with negative c (b) has been also discussed.

The coupling constant of scalar field is fixed by the standard (for the NJL model) relation between the quark mass and the π-meson decay constant $g_\sigma = M/f_\pi$ (we put $f_\pi = 100$ MeV) although there is no any objection to treat this coupling constant as an independent parameter. As a result of all agreements done we have for the σ-meson mass $m_\sigma = g_\sigma\ M/C_s$. In principle, we could even fix the σ-meson mass and coupling constant g_σ but all relations above mentioned lead eventually to quite suitable values of the σ-meson mass as will be demonstrated below.

The vector field plays, as we see, a secondary role because of the small magnitude of constant C_v. Then taking the vector meson mass as $m_v \approx 740$ MeV (slightly smaller than the mass of ω-meson because of simple technical reason only) we calculate the coupling constant of vector field from the relation similar to the scalar field $m_v = g_v\ M/C_v$. Amazingly, its value comes about steadily small in comparing to the value characteristic for the NJL model $g_v = \sqrt{6} g_\sigma$. However, at the values of constant C_v which we are interested in it is very difficult to maintain the reasonable balance and for the sake of clarity we prefer to choose the massive vector field. Actually, it is unessential because we need this parameter (as we remember) only to estimate the vector field strength.

The key point of our interest here is the surface tension coefficient [16] which can be defined as

$$u_s = 4\pi\ r_o^2 \int_{-\infty}^{\infty} dx\ \left[\mathcal{E}(x) - \frac{\mathcal{E}_l}{\rho_l}\ \rho(x)\right] . \qquad (33)$$

The parameter r_o will be discussed in the next section at considering the features of quark liquid droplet, and for the present we would like to notice only that for the parameters considered its magnitude for $N_f = 1$ is around $r_o = 0.79$ fm. Recalling the factor $3^{1/3}$ which connects the baryon and quark numbers one can find the magnitude ($\widetilde{r}_o = 3^{1/3} 0.79 \approx 1.14$ fm) is in full agreement with the magnitude standard for the nuclear matter calculations (in the Walecka model) $\widetilde{r}_o = 1.1 - 1.3$ fm.

In order to proceed we calculate $\mathcal{E}(x)$ in the Thomas–Fermi approximation as

$$\mathcal{E}(x) \ = \ \gamma \int^{P_F(x)} \frac{d\mathbf{p}}{(2\pi)^3}\ [\mathbf{p}^2 + \overset{*}{M}(x)]^{1/2} + \\ + \ \frac{1}{2}\ g_v\ \rho(x)\ V(x) - \frac{1}{2}\ g_\sigma\ \rho_s(x)\ \sigma(x)\ .$$

And to give some idea for the 'setup' prepared we present here the characteristic parameter values for some fixed b and c with $\rho_l = 3 \times 0.157$ ch/fm^3. In the liquid phase they are $\overset{*}{M}= 70$ MeV ($P_F = 327$ MeV) and $e_l = 310.5$ MeV (index l stands for a liquid phase and $e(x) = \mathcal{E}(x)/\rho(x)$ defines the density of specific energy). Both equations (31) and (32) are obeyed by this state. There exist the solution with larger value of quark mass $\overset{*}{M}= 306$ MeV,

(P_F = 135 MeV) (we have faced the similar situation in the first section dealing with the gas of quark quasiparticles) and $e = 338$ MeV $\sim e_g$ (e_g is the specific energy in the gas phase) which satisfies both equations as well. The specific energy of this solution occurs to be larger than specific energy of the previous solution. It is worthwhile to mention the existence of intermediate state corresponding to the saturation point with the mass $\overset{*}{M}$= 95 MeV, (P_F = 291 MeV) and e = 306 MeV. Obviously, it is the most favorable state with the smallest value of specific energy (and with the zero pressure of quark ensemble), and the system can reach this state only in the presence of significant vector field. This state (already discussed in the first section) corresponds to the minimal value of chemical potential ($T = 0$) and can be reached at the densities typical for the normal nuclear matter. However, Eq. (32) is not valid for this state.

Two another parameters η, ζ are fixed by looking through all the configurations in which the solution of equation system (28) with stable kink of the scalar field does exist and describes the transition of the gas phase quarks to the liquid phase. First, it is reasonable to scan the η, c ($\zeta = c\ \eta$)-plane, in order to identify the domain in which the increase of specific energy $\mathcal{E} - \mathcal{E}_l\ \rho/\rho_l \leq 0$ is revealed at running through all possible states which provide the necessary transition (without taking into account the field gradients). In practice one need to follow a simple heuristic rule. The state with $P_F \sim 1$ MeV (i.e. e and the corresponding ρ). The state of characteristic liquid energy $\mathcal{E}_l$ (together with ρ_l) should be compared at scanning the Lagrangian parameters η and c. Just this domain where they are commensurable could provide us with the solutions in which we are interested and Fig.7 shows its boundary. The curve could be continued beyond the value $\eta = 2.5$ but the values of corresponding parameter η are unrealistic and not shown in the plot.

We calculate the solution of equation system (28) numerically by the Runge–Kutta method with the initial conditions $\sigma(L) \approx 0$, $\sigma'(L) \approx 0$ imposed at the large distance $L \gg t$ where t is a characteristic thickness of transition layer (about 2 fm). Such a simple algorithm occurs quite suitable if the vector field contribution is considered as a small correction (what just takes place in the situation under consideration) and is presented as

$$V(x) = \frac{1}{2m_v} \int_{-L}^{L} dz\ e^{-m_v|x-z|}\ g_v\ \rho(z)\ ,$$

where the charge (density) ρ is directly defined by the scalar field. We considered the solutions including the contribution of the vector field as well and the corresponding results confirm the estimates obtained.

Rather simple analysis shows the interesting solutions are located along the boundary of discussed domain. Some of those are depicted in Fig. 7 as the dots. Fig. 8 shows the stable kinks of σ-field with the parameter $c = 1.1$ for two existing solutions with $\eta \approx 0.977$ ($m_\sigma \approx 468$ MeV) (solid line) and $\eta \approx 1.813$ ($m_\sigma \approx 690$ MeV) (dashed line). For the sake of clarity we consider the gas (vacuum) phase is on the right. Then the asymptotic value of σ-field on the left hand side ($\sigma \approx 80$ MeV) corresponds to $\overset{*}{M}$= 70 MeV. The thickness of transition layer for the solution with $\eta \approx 0.977$ is $t \approx 2$ fm while for the second solution $t \approx 1$ fm.

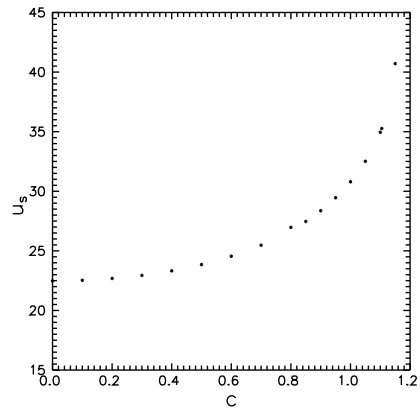

FIG. 9: The surface tension coefficient u_s in MeV as a function of parameter c ($\zeta = c\ \eta$) for the curve of stable kinks (with $\eta \leq 1.2$).

Characterizing the whole spectrum of the solutions obtained we should mention that there exist another more rigid (chiral) kinks which correspond to the transition into the state with the dynamical quark mass changing its sign, i.e. $M \to -M$. In particular, the kink with the canonical parameter values $\eta = 1$, $c = 1$ is clearly seen (marked by the star in Fig. 7) and its surface tension coefficient is about $2m_\pi$ (m_π is the π-meson mass). The most populated class of solutions consists of those having the meta-stable character. The system comes back to the starting point (after an evolution) pretty rapidly, and usually the σ-field does not evolve in such an extent to reach the asymptotic value (which corresponds to the dynamical quark mass in the liquid phase $\overset{*}{M}$= 70 MeV). Switching on the vector field changes the solutions insignificantly (for our situation with small C_v it does not exceed 2 MeV in the maximum).

The surface tension coefficient u_s in MeV for the curve of stable kinks with parameter $\eta \leq 1.2$ as the function of parameter c ($\zeta = c\ \eta$) is depicted in Fig. 9. The σ-meson mass at $c \approx 0$ is $m_\sigma \approx 420$ MeV and changes smoothly up to the value $m_\sigma \approx 500$ MeV at $c \approx 1.16$ (the maximal value of the coefficient c beyond which the stable kink solutions are not observed). In particular, $m_\sigma \approx 450$ MeV at $c = 1$. Two kink solutions with $c = 1.1$ for $\eta \approx 0.977$ and for $\eta \approx 1.813$ (shown in Fig. 8, and the second one is not shown in Fig. 9) have the tension coefficient values $u_s \approx 35$ MeV and $u_s \approx 65$ MeV, correspondingly. The maximal value of tension coefficient for the normal nuclear matter does not exceed $u_s = 50$ MeV. The nuclear Walecka model claims the value $u_s \approx 19$ MeV [16] as acceptable and calculable. The reason to have this higher

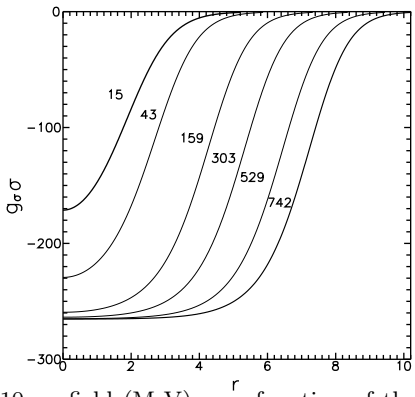

FIG. 10: σ-field (MeV) as a function of the distance r (fm) for several solutions of the equation system (28) which are characterized by the net quark number N_q written to the left of each curve.

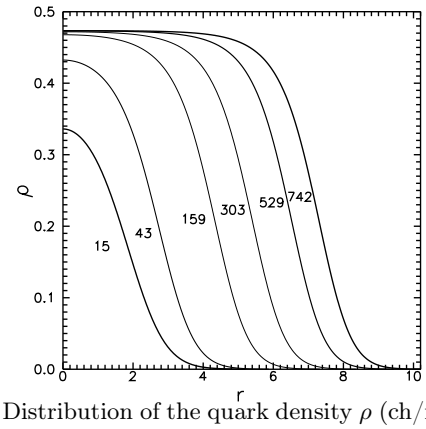

FIG. 11: Distribution of the quark density ρ (ch/fm^3) for the corresponding solutions presented in Fig. 11.

value of surface tension coefficient for quarks is rooted in the different magnitudes of the mass deficit. Indeed, for nuclear matter it does not exceed $\overset{*}{M}\approx 0.5M$ albeit more realistic values are considered around $\overset{*}{M}\approx 0.7M$ and for the quark ensemble the mass deficit amounts to $\overset{*}{M}\approx 0.3M$. We are also able to estimate the compression coefficient of quark matter K which occurs significantly larger than the nuclear one. Actually, we see quite smooth analogy between the results of Section II and the results of bag soliton model [17]. The thermodynamic treatment developed in the present paper allows us to formulate the adequate boundary conditions for the bag in physical vacuum and to diminish considerably the uncertainties in searching the true soliton Lagrangian. We believe it was also shown here that to single out one soliton solution among others (including even those obtained by the exact integration method [14]), which describes the transitional layer between two media, is not easy problem if the boundary conditions above formulated are not properly imposed.

III. DROPLET OF QUARK LIQUID

The results of two previous sections have led us to put the challenging question about the creation and properties of finite quark systems or the droplets of quark liquid which are in equilibrium with the vacuum state. Thus, as a droplet we imply the spherically-symmetric solution of the equation system (28) for $\sigma(r)$ and $V(r)$ with the obvious boundary conditions $\sigma'(0) = 0$ and $V'(0) = 0$ in the origin (the primed variables denote the first derivatives in r) and rapidly decreasing at the large distances $\sigma \to 0$, $V \to 0$, when $r \to \infty$.

A quantitative analysis of similar nuclear physics models which includes the detailed tuning of parameters is usually based on the comprehensive fitting of available experimental data. This way is obviously irrelevant in studying the quark liquid droplets. This global difficulty dictates a specific tactics of analyzing. We propose to start, first of all, with selecting the parameters which could be worthwhile to play a role of physical observables. Naturally, the total baryon number which phenomenologically (via factor 3) related to the number of valence quark in an ensemble is a reasonable candidate for this role. Besides, the density of quark ensemble $\rho(r)$, the mean size of droplet R_0 and the thickness of surface layer t look suitable for such an analysis.

It is argued above that the vector field contribution is negligible because of the smallness of the coefficient C_v comparing to the C_s magnitude, and we follow this conclusion (or assumption) albeit understand it is scarcely justified in the context of finite quark system. Thus, we will put $g_v = 0$, $V = 0$ in what follows and it will simplify all the calculations enormously.

Fig. 10 shows the set of solutions (σ-field in MeV) of the system (28) at $N_f = 1$ and Fig. 11 presents the corresponding distributions of ensemble density ρ (ch/fm^3). The parameters C_s, C_v, b and c are derived by the same algorithm as in the previous section, i.e. the chemical potential of quark ensemble $M = 335$ МэВ (and $\sigma \to 0$) is fixed at the spatial infinity. The filled-up states (liquid) are characterized by the parameters $\overset{*}{M}= 70$ MeV, $\rho_0 = \rho_l = 3 \times 0.157$ ch/fm^3. The σ-meson mass and the coupling constant g_σ are derived at fixed coefficients η and ζ, and they just define the behaviour of solutions $\sigma(r)$, $\rho(r)$, etc. The magnitudes of functions $\sigma(r)$ and $\rho(r)$ at origin are not strongly correlated with the values characteristic for the filled-up states and are practically determined by solving the boundary value problem for system (28). In particular, the solutions presented in Fig. 10 have been received with the running coefficient η at $\zeta = \eta$. The most relevant parameter (instead of η) from the physical view point is the total number of quarks in the droplet N_q (as discussed above) and it is depicted to the left of each curve. (The variation of $\overset{*}{M}$, ρ_0 and f_π could be considered as well instead of two mentioned parameters η and ζ.)

TABLE I: Results of fitting by the Fermi distribution with $N_f = 1$, $\widetilde{\rho}_0$ (ch/fm^3), R_0, t, r_0 (fm), b (fm^{-1}), m_σ (MeV).

N_q	$\widetilde{\rho}_0$	R_0	b	t	r_0	m_σ	η
15	0.34	1.84	0.51	2.24	0.74	351	0.65
43	0.43	2.19	0.52	2.28	0.75	384	0.73
159	0.46	4.19	0.52	2.29	0.77	409	0.78
303	0.47	5.23	0.52	2.29	0.78	417	0.795
529	0.47	6.37	0.52	2.27	0.79	423	0.805
742	0.47	7.15	0.52	2.27	0.79	426	0.81

TABLE II: Results of fitting by the Fermi distribution with $N_f = 2$, $\widetilde{\rho}_0$ (ch/fm^3), R_0, t, r_0 (fm), b (fm^{-1}), m_σ (MeV).

N_q	$\widetilde{\rho}_0$	R_0	b	t	r_0	m_σ	η
18	0.81	1.56	0.37	1.63	0.57	524	0.7
46	0.9	2.14	0.37	1.63	0.6	557	0.75
169	0.93	3.43	0.36	1.6	0.62	586	0.79
278	0.94	4.08	0.36	1.6	0.62	594	0.8
525	0.94	5.04	0.36	1.6	0.62	603	0.81
776	0.94	5.76	0.36	1.6	0.63	607	0.815

Analyzing the full spectrum of solutions obtained by scanning one can reveal a recurrent picture (at a certain scale) of kink-droplets which are easily parameterized by the total number of quarks N_q in a droplet and by the density ρ_0. These characteristics are evidently fixed at completing the calculations. The sign which allows us to single out these solutions is related to the value of droplet specific energy (see below).

Table I exhibits the results of fitting the density $\rho(r)$ with the Fermi distribution

$$\rho_F(r) = \frac{\widetilde{\rho}_0}{1 + e^{(R_0 - r)/b}} \ , \tag{34}$$

where $\widetilde{\rho}_0$ is the density in origin, R_0 is the mean size of droplet and the parameter b defines the thickness of surface layer $t = 4\ln(3)b$. Besides, the coefficient r_0 which is absorbed in the surface tension coefficient (33), the σ-meson mass, $R_0 = r_0 N_q^{1/3}$ and the coefficient η at which all other values have been obtained are also presented in the Table I.

The curves plotted in the Fig. 10 and results of Table I allows us to conclude that the density distributions at $N_q \geq 50$ are in full agreement with the corresponding data typical for the nuclear matter. The thicknesses of transition layers in both cases are also similar and the coefficient r_0 with the factor $3^{1/3}$ included is in full correspondence with $\widetilde{r}_0$. The values of σ-meson mass in Table I look quite reasonable as well. However the corresponding quantities are strongly different at small quark numbers in the droplet. We know from the experiments that in the nuclear matter some increase of the nuclear density is observed. It becomes quite considerable for the Helium and is much larger than the standard nuclear density for the Hydrogen.

Obviously, we understand the Thomas–Fermi approximation which is used for estimating becomes hardly justified at small number of quarks, and we should deal with the solutions of complete equation system (28). However, one very encouraging hint comes from the chiral soliton model of nucleon [18], where it has been demonstrated that solving this system (28) the good description of nucleon and Δ can be obtained. Then our original remark could be that the soliton solutions obtained in [18] permit an interpretation as a 'confluence' of two kinks. Each of those kinks 'works' on the restoration of chiral symmetry since the scalar field approaches its zero value at the distance of ~ 0.5 fm from the kink center. Indeed, one branch of our solution corresponds the positive value of dynamical quark mass, and another branch presents the solution with negative dynamical quark mass (in three-dimensional picture the pseudo-scalar fields appear just as a phase of chiral rotation from positive to negative value of quark mass). Such solutions develop the surface tension coefficient which is larger in factor two than the corresponding coefficient of single kink and as we believe signal some instability of a single kink solution.

The similar results are obtained for two flavours $N_f = 2$ ($\gamma = 2N_f N_c = 12$) assuming all dynamical quark masses of SU(2) flavour multiplet are equal. The solutions for the σ-field and density distributions are similar to the corresponding results presented in Fig. 10 and Fig. 11. The other data of fitting solutions are shown in the following Table II. As it is seen the characteristic ensemble density is approximately in factor two larger than the density of normal nuclear matter (remember again the factor 3). The characteristic values of σ-meson mass are slightly larger than for $N_f = 1$ and, consequently, the thickness of the transition layer is smaller almost in factor 1.4. The coefficient interrelating the mean size of droplet and the baryon (quark) number $\widetilde{r}_0 \sim 0.8$ is getting smaller. In principle, one can correct (increase) the surface layer thickness and the parameter $\widetilde{r}_0$ by decreasing the σ-meson mass but the ensemble density remains higher than the normal nuclear one.

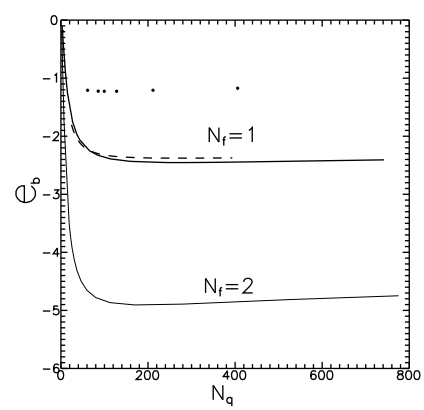

FIG. 12: The specific binding energy at $N_f = 1$ and $N_f = 2$ in MeV as a function of quark number N_q.

Fig. 12 displays the specific binding energy of ensemble. It is defined by the expression similar to Eq. (33) in which the integration over the quark droplet volume is performed. The specific energy is normalized (compared) to the ensemble energy at the spatial infinity, i.e. in vacuum. Actually, Fig. 12 shows several curves in the upper part of plot which correspond the calculations with $N_f = 1$. The solid line is obtained by scanning over parameter η and corresponds to the data presented in Table I. The dashed curve is calculated at fixed $\eta = 0.4$ but by scanning over parameter $\overset{*}{M}$. It is clearly seen if the specific energy data are presented as a function of quark number N_q then the solutions, in which we are interested, rally in the local vicinity of the curve where the maximal binding energy $-|\mathcal{E}_b|$ is reached.

The similar solution scanning can be performed over the central density parameter ρ_0 in origin. The corresponding data are dotted for a certain fixed $\overset{*}{M}$ and ρ_0. It is interesting to notice that at scanning over any variable discussed a saturation property is observed and it looks like the minimum in e_b at $N_q \sim$ 200–250. The results for the specific binding energy as a function of particle number are in the qualitative agreement with the corresponding experimental data. And one may say even about the quantitative agreement if the factor 3 (the energy necessary to remove one baryon) is taken into account. Another interesting fact to be mentioned is that there exist the solutions of system (28) with positive specific energy. For example, for $N_f = 2$ such meta-stable solutions appear at sufficiently large η and with the density parameter in origin equal $\rho_0 \sim \rho_l = 0.157\,\mathrm{ch/fm}^3$. In fact, the equation system (28) represents an equation of balance for the current quarks circulating between liquid and gas phases.

As a conclusion we would like to emphasize that in the present paper we have demonstrated how a phase transition of liquid–gas kind (with the reasonable values of parameters) emerges in the NJL-type models. The constructed quark ensemble displays some interesting features for the nuclear ground state (for example, an existence of the state degenerate with the vacuum one), and the results of our study are suggestive to speculate that the quark droplets could coexist in equilibrium with vacuum under the normal conditions. These droplets manifest themselves as bearing a strong resemblance to the nuclear matter. Elaborating this idea in detail is a great challenge which will take a lot of special efforts and we do hope to undertake them in near future.

Authors are deeply indebted K. A. Bugaev, R. N. Faustov, S. B. Gerasimov, E.-M. Ilgenfritz, K. G. Klimenko, E. A. Kuraev, A. V. Leonidov, V. A. Petrov, A. M. Snigirev and many other colleagues for numerous fruitful discussions.

Appendix A: Mean energy functional

The free part of Hamiltonian

$$H_0 = -\int d\mathbf{x}\ \bar{q}(\mathbf{x})\ (i\gamma\nabla + im)\ q(\mathbf{x}) =$$
$$= \int \frac{d\mathbf{p}}{(2\pi)^3}|p_4|\left[\cos\theta\left(A^+(\mathbf{p};s)A(\mathbf{p};s) - B(\mathbf{p};s)B^+(\mathbf{p};s)\right) + \right.$$
$$\left. + \sin\theta\left(A^+(-\mathbf{p};s)B^+(\mathbf{p};s) + B(-\mathbf{p};s)A(\mathbf{p};s)\right)\right],$$

contributes into the mean energy as

$$\mathrm{Tr}\{\xi\ \mathcal{H}_0\} = \int \frac{d\mathbf{p}}{(2\pi)^3}\ |p_4|\ (1-\cos\theta) + \\ + \int \frac{d\mathbf{p}}{(2\pi)^3}\ |p_4|\cos\theta\ [n(p) + \bar{n}(p)]\ , \tag{A1}$$

where $\mathcal{H}_0 = H_0/(V2N_c)$ is the specific energy. Natural regularization by subtracting the free Hamiltonian H_0 contribution (without pairing quarks and anti-quarks) has been done in the first term of Eq. (A1) because in our particular situation this normalization in order to have the ensemble energy equal zero at the pairing angle equal zero turns out quite practical. It just explains a presence of unit in the term containing $\cos\theta$.

The Hamiltonian part responsible for interaction, $\bar{q}t^a\gamma_\mu q\bar{q}'t^a\gamma_\nu q'$, provides four nontrivial contributions. The term $\mathrm{Tr}\{\rho BB^+B'B'^+\}$ generates the following items: $\overline{V}_{\alpha i}(\mathbf{p},s)t^a_{ij}\gamma^\mu_{\alpha\beta}V_{\beta j}(\mathbf{Q},T)\overline{V}_{\gamma k}(\mathbf{Q},T)t^b_{kl}\gamma^\mu_{\gamma\delta}V_{\delta l}(\mathbf{p},s)$ (the similar term but with the changes $Q,T \to Q',T'$ which generates another primed quark current should be added) and $-2\overline{V}(\mathbf{Q},T)\ \ t^a\gamma^\mu V(\mathbf{Q}',T')\overline{V}(\mathbf{Q}',T')t^b\gamma^\mu V(\mathbf{Q},T)$. Here (as in all other following expressions) we omitted all colour and spinor indices which are completely identical to those of previous matrix element. The term $\mathrm{Tr}\{\rho BAA'^+B'^+\}$ generates the following nontrivial contributions: $\overline{V}(\mathbf{p},s)t^a\gamma^\mu U(\mathbf{q},t)\overline{U}(\mathbf{q},t)t^b\gamma^\mu V(\mathbf{p},s)$ $-\overline{V}(\mathbf{p},s)t^a\gamma^\mu U(\mathbf{P},S)\overline{U}(\mathbf{P},S)t^b\gamma^\mu V(\mathbf{p},s)$ $-\overline{V}(\mathbf{Q},T)t^a\gamma^\mu U(\mathbf{q},t)\overline{U}(\mathbf{q},t)t^b\gamma^\mu V(\mathbf{Q},T)$ $+\overline{V}(\mathbf{Q},T)t^a\gamma^\mu U(\mathbf{P},S)\overline{U}(\mathbf{P},S)t^b\gamma^\mu V(\mathbf{Q},T)$. Averaging $\mathrm{Tr}\{\rho AA^+A'A'^+\}$ gives the contributions as: $\overline{U}(\mathbf{P},S)t^a\gamma^\mu U(\mathbf{p},s)\overline{U}(\mathbf{p},s)t^b\gamma^\mu U(\mathbf{P},S)$ (adding the similar term but with the changes $P,S \to P',S'$) and $-2\overline{U}(\mathbf{P},S)t^a\gamma^\mu U(\mathbf{P}',S')\overline{U}(\mathbf{P}',S')t^b\gamma^\mu V(\mathbf{P},S)$. Another nontrivial contribution comes from averaging $\mathrm{Tr}\{\rho A^+B^+B'A'\}$ and it has the form $\overline{V}(\mathbf{Q},T)t^a\gamma^\mu U(\mathbf{P},S)\overline{U}(\mathbf{P},S)t^b\gamma^\mu V(\mathbf{Q},T)$. All other diagonal matrix elements generated by the following terms $\mathrm{Tr}\{\rho AA^+B'B'^+\}$, $\mathrm{Tr}\{\rho BB'^+A'^+A'\}$, do not contribute at all (their contributions equal to zero). Similar to the calculation of matrix elements at zero temperature performed in Ref. [5] we should carry out the integration over the Fermi sphere with the corresponding distribution functions in the quark and anti-quark momenta $\int^{P_F}\frac{d\mathbf{p}}{(2\pi)^3} \to \int\frac{d\mathbf{p}}{(2\pi)^3}[n(p)+\bar{n}(p)]$ if deal with a finite temperature. All necessary formulae for the polarization matrices which contain the traces of

corresponding spinors could be found in Refs. [4] and [5]. Bearing in mind this fact here we present immediately the result for mean energy density per one quark degree of freedom as

$$
\begin{aligned}
w \;=\; & \int \frac{d\mathbf{p}}{(2\pi)^3}|p_4|\cos\theta[n(p)+\bar{n}(p)] + 2G\int \frac{d\mathbf{p}}{(2\pi)^3}\sin(\theta-\theta_m)\,[n(p)+\bar{n}(p)]\int \frac{d\mathbf{q}}{(2\pi)^3}\sin(\theta'-\theta'_m)\,I - \\
- \; & G\int \frac{d\mathbf{p}}{(2\pi)^3}\;\sin(\theta-\theta_m)\,[n(p)+\bar{n}(p)]\int \frac{d\mathbf{q}}{(2\pi)^3}\;\sin(\theta'-\theta'_m)\;\;[n(q)+\bar{n}(q)]\;I + \\
+ \; & \int \frac{d\mathbf{p}}{(2\pi)^3}\;|p_4|(1-\cos\theta) - G\int \frac{d\mathbf{p}}{(2\pi)^3}\;\sin(\theta-\theta_m)\int \frac{d\mathbf{q}}{(2\pi)^3}\;\sin(\theta'-\theta'_m)\;\;I\;,
\end{aligned}
\tag{A2}
$$

(up to the constant unessential for our consideration here)[23]. It is quite practical to single out the colour factor in the four-fermion coupling constant as $G = 2\widetilde{G}/N_c$. Performing now the following transformations while integrating in the interaction terms

$$
\begin{aligned}
& 2\int d\mathbf{p}\;f\int d\mathbf{q} - \int d\mathbf{p}\;f\int d\mathbf{q}\;f' - \int d\mathbf{p}\int d\mathbf{q} = \\
& = \int d\mathbf{p}\;f\int d\mathbf{q}\;(1-f') - \int d\mathbf{p}\;(1-f)\int d\mathbf{q},
\end{aligned}
$$

and changing the variables $\mathbf{p} \leftrightarrow \mathbf{q}$ in the last term we obtain

$$
\begin{aligned}
& \int d\mathbf{p}\;f\int d\mathbf{q}\;(1-f') - \int d\mathbf{p}\int d\mathbf{q}\;(1-f') = \\
& -\int d\mathbf{p}\;(1-f)\int d\mathbf{q}\;(1-f')\;.
\end{aligned}
$$

Here the primed variables correspond to the momentum q. Then putting all the terms together we come to the equation (11).

[1] J. Wambach, arXiv:1101.4760v1 [hep-ph].
[2] N. Borghini, Heavy ions at the LHC: lessons from the first data. Talk given at the LHCC meeting at CERN on March 4, 2011.
[3] V. A. Khodel, Pis'ma JETF, **16**, 410 (1972); **18**, 126 (1973); S. A. Fayans, V. A. Khodel, Pis'ma JETF, **17**, 633 (1973).
[4] G. M. Zinovjev and S. V. Molodtsov, Teor. Mat. Fiz. **160**, 244 (2009); Phys. Rev. **D80**, 076001 (2009); Europhys. Lett. **93**, 11001 (2011).
[5] S. V. Molodtsov, A. N. Sissakian and G. M. Zinovjev, Europhys. Lett. **87**, 61001 (2009); Phys. of Atomic Nucl., **73**, 1245 (2010).
[6] Y. Nambu and G. Jona-Lasinio, Phys. Rev. **122**, 345 (1961).
[7] T. Hatsuda and T. Kunihiro, Phys. Rep. **247**, 221 (1994).
[8] H. Tezuka, Phys. Rev. **C22**, 2585 (1980); **C24**, 288 (1981).
[9] T. Matsui, Nucl. Phys. **A370**, 369 (1981).
[10] M. Asakawa and K. Yazaki, Nucl. Phys. **A504**, 668 (1989).
[11] L. Ya. Glozman, Phys. Rep. **444**, 1 (2007).
[12] A. I. Larkin, Yu. N. Ovchinnikov, JETF, **47**, 1136 (1964).
[13] T. Eguchi and H. Sugawara, Phys. Rev. **D10**, 4257 (1974); K. Kikkawa, Prog. Theor. Phys. **56**, 947 (1976); M. K. Volkov, PEPAN, **17**, 433 (1986).
[14] S. Carignano, D. Nickel and M. Buballa, arXiv:1007.1397 [hep-ph]; D. Nickel, Phys. Rev. Lett. **103**, 072301 (2009); G. Basar and G. V. Dunne, Phys. Rev. Lett. **100**, 200404 (2008); T. Kunihiro, Y. Minami and Z. Zhang, arXiv:1009.4534 [nucl-th].
[15] J. D. Walecka, Annals of Phys. **83**, 491 (1974); F. E. Serr and J. D. Walecka, Phys. Lett. **B79**, 10 (1978).
[16] J. Boguta and A. Bodmer, Nucl. Phys. **A292**, 413 (1977).
[17] K. Huang and D. R. Stump, Phys. Rev. **D14**, 223 (1976); R. Friedberg and T. D. Lee, Phys. Rev. **D18**, 2623 (1978); R. Goldflam and L. Wilets, Phys. Rev. **D25**, 1951 (1982); E. G. Lübeck, M. C. Birse, E. M. Henley, and L. Wilets, Phys. Rev. **D33**, 234 (1986).
[18] W. Broniowski and M. K. Banerjee, Phys. Lett. **B158**, 335 (1978).
[19] At the Fermi momenta of dynamical quark mass order.
[20] The chiral quark condensate for the filled up state develops the quantity about (100 MeV)^3 (at $T = 0$), see [5], that demonstrates the obvious tendency of restoring a chiral symmetry.
[21] Indirect confirmation of this hypothesis one could observe, for example, in the existing degeneracy of excited baryon states Ref. [11].
[22] Similar uncertainty is present in the other predictions of chiral symmetry restoration scenarios, for example, it stretches from 2 till 6 units of the normal nuclear density.

[23] It is interesting to notice that the existence of the angle θ_m stipulates the discontinuity of mean energy functional mentioned above and discovered in [4].